



LAWRENCE
LIVERMORE
NATIONAL
LABORATORY

UCRL-CONF-200711

An Investigation of Implicit Active Contours for Scientific Image Segmentation

S.K. Weeratunga, C. Kamath

November 5, 2003

Visual Communications and Image Processing Conference,
IS&T/SPIE Symposium Electronic Imaging, San Jose, CA,
January 18-22, 2004.

This document was prepared as an account of work sponsored by an agency of the United States Government. Neither the United States Government nor the University of California nor any of their employees, makes any warranty, express or implied, or assumes any legal liability or responsibility for the accuracy, completeness, or usefulness of any information, apparatus, product, or process disclosed, or represents that its use would not infringe privately owned rights. Reference herein to any specific commercial product, process, or service by trade name, trademark, manufacturer, or otherwise, does not necessarily constitute or imply its endorsement, recommendation, or favoring by the United States Government or the University of California. The views and opinions of authors expressed herein do not necessarily state or reflect those of the United States Government or the University of California, and shall not be used for advertising or product endorsement purposes.

An investigation of implicit active contours for scientific image segmentation

Sisira K. Weeratunga and Chandrika Kamath

Lawrence Livermore National Laboratory, 7000 East Avenue, Livermore, CA 94551

ABSTRACT

The use of partial differential equations in image processing has become an active area of research in the last few years. In particular, active contours are being used for image segmentation, either explicitly as snakes, or implicitly through the level set approach. In this paper, we consider the use of the implicit active contour approach for segmenting scientific images of pollen grains obtained using a scanning electron microscope. Our goal is to better understand the pros and cons of these techniques and to compare them with the traditional approaches such as the Canny and SUSAN edge detectors. The preliminary results of our study show that the level set method is computationally expensive and requires the setting of several different parameters. However, it results in closed contours, which may be useful in separating objects from the background in an image.

Keywords: level set, implicit active contour, image segmentation, edge detection

1. INTRODUCTION

Techniques based on partial differential equations are increasingly being used in image processing for tasks such as noise reduction, segmentation, registration, and object tracking.^{1,2} In this paper, we focus on the use of implicit active contours for image segmentation. Implicit active contours, also known as level set techniques, have been the subject of active research in the last few years. The use of these techniques is being explored in a variety of applications including medical image segmentation in two- and three-dimensions, motion analysis, and image registration.³⁻⁶

The idea behind active contours, or deformable models, for image segmentation is quite simple. The user specifies an initial guess for the contour, which is then moved by image driven forces to the boundaries of the desired objects. In such models, two types of forces are considered - the internal forces, defined within the curve, are designed to keep the model smooth during the deformation process, while the external forces, which are computed from the underlying image data, are defined to move the model toward an object boundary or other desired features within the image.

There are two forms of deformable models. In the parametric form, also referred to as snakes, an explicit parametric representation of the curve is used. This form is not only compact, but is robust to both image noise and boundary gaps as it constrains the extracted boundaries to be smooth. However, it can severely restrict the degree of topological adaptability of the model, especially if the deformation involves splitting or merging of parts. In contrast, the implicit deformable models, also called implicit active contours or level sets, are designed to handle topological changes naturally. However, unlike the parametric form, they are not robust to boundary gaps and suffer from several other deficiencies as well.⁷

In this paper, we present some preliminary results obtained using the implicit active contour for the segmentation of scientific images, in particular, scanning electron microscope (SEM) images of pollen. Our main goal here is to compare one of the recently proposed PDE-based techniques for image segmentation⁸ with some of the more traditional approaches such as the Canny⁹ and the SUSAN¹⁰ edge detectors, in order to better understand the pros and cons of each approach.

Further author information: (Send correspondence to C.K.)

C.K.: Center for Applied Scientific Computing, L-561, P.O. Box 808, Lawrence Livermore National Laboratory, Livermore, CA 94551, U.S.A. E-mail: kamath2@llnl.gov

This paper is organized as follows: in Section 2, we provide an overview of the implicit active contour method and discuss the details of our implementation. Next, in Section 3, we describe the two traditional segmentation techniques, i.e., Canny and SUSAN, which we use for comparison. Section 4 describes the test images and the results from the different segmentation techniques. Finally, in Section 5, we conclude with a summary and our plans for future work.

2. OVERVIEW OF IMPLICIT ACTIVE CONTOURS

The implicit active contour, or level set, approach was introduced by Osher and Sethian¹¹ and has since been enhanced by several authors.³⁻⁶ An easy-to-understand high-level description of the level set method is given in.¹² The basic idea is to start with a closed curve in two dimensions (or a surface in three dimensions) and allow the curve to move perpendicular to itself at a prescribed speed. One way of describing this curve is by using an explicit parametric form, which is the approach used in snakes. As mentioned earlier, this causes difficulties when the curves have to undergo splitting or merging, during their evolution to the desired shape. To address this difficulty, the implicit active contour approach, instead of explicitly following the moving interface itself, takes the original interface and embeds it in higher dimensional scalar function, defined over the entire image. The interface is now represented implicitly as the zero-th level set (or contour) of this scalar function. Over the rest of the image space, this level set function ϕ is defined as the signed distance function from the zero-th level set. Specifically, given a closed curve C_0 , the function is zero if the pixel lies on the curve itself, otherwise, it is the signed minimum distance from the pixel to the curve. By convention, the distance is regarded as negative for pixels inside C_0 and positive for pixels outside C_0 . The function ϕ , which varies with space and time (that is, $\phi = \phi(x, y, t)$ in two dimensions) is then evolved using a partial differential equation (PDE), containing terms that are either hyperbolic or parabolic in nature.

In order to illustrate the origins of this PDE, we next consider the evolution of the function ϕ as it evolves in a direction normal to itself with a known speed F . Here, the normal is oriented with respect to an outside and an inside. Since the evolving front is a zero level set (i.e., a contour with value 0) of this function, we require (using a one-dimensional example)

$$\phi(x(t), t) = 0$$

for any point $x(t)$ on the zero level set at time t . Using the chain rule, we have

$$\phi_t + \nabla\phi(x(t), t) \cdot x'(t) = 0$$

Since F is the speed in the direct n normal to the curve, we have

$$x'(t) \cdot n = F$$

where

$$n = \frac{\nabla\phi}{\|\nabla\phi\|}$$

Thus, the evolution of ϕ can be written as

$$\phi_t + F\|\nabla\phi\| = 0 \tag{1}$$

where $\phi(x, t = 0)$, that is, the curve at time $t = 0$, is given. This formulation enables us to handle topological changes as the zero level set need not be a single curve, but can easily split and/or merge as t advances.

Equation (1) can be solved using appropriate finite difference approximations for the spatial and temporal derivatives¹³ and considering the image pixels to be a discrete grid in the $x - y$ domain with uniform mesh spacing. In order to evolve the level set, we need the specification of an initial closed curve(s), the initialization of the signed distance function ϕ over the rest of the image, the finite difference discretization of Eqn. (1), and the prescription of the propagation speed F . We next discuss each of these issues in detail.

2.1. Choice of the speed function F

The speed F depends on many factors including the local properties of the curve, such as the curvature, and the global properties, such as the shape and the position of the front. It can be used to control the front in several different ways. The original level set method proposed using F as the sum of two terms

$$F = F_0 + F_1(\kappa)$$

where F_0 is a constant propagation term and F_1 is a scalar function of the curvature κ

$$\kappa = \operatorname{div}\left(\frac{\nabla\phi}{\|\nabla\phi\|}\right)$$

The propagation term F_0 , sometimes referred to as the ‘‘balloon force’’, is independent of the geometry of the moving front and the front uniformly expands or contracts with speed F_0 , depending on its sign.¹⁴ Note that the F_0 term is hyperbolic, while the F_1 term is parabolic. The key idea is to play one term against the other - the hyperbolic term leads to the formation of shocks from which a representation of the shape can be deduced, while the curvature term smooths the front, which enables us to distinguish the more significant shape features from the less significant ones.^{14, 15}

Since we are using level sets for image segmentation, we want the zero-th level set to stop evolving at an edge in the image. This can be accomplished by multiplying the speed term by an image-dependent stopping factor $g(x, y)$ given by the following equation:

$$g(x, y) = 1/\left(1 + \frac{|\nabla I_\sigma|^2}{\lambda^2}\right) \quad (2)$$

where I_σ is the image I convolved with a Gaussian defined as follows:

$$G_\sigma(x, y) = \frac{1}{2\pi\sigma^2} \exp\left(-\frac{|x|^2 + |y|^2}{2\sigma^2}\right) \quad (3)$$

Equation (2) is the the one used by Perona and Malik in their work on smoothing images using the diffusion equation.¹⁶ In the original work, this term was used to stop the diffusion process near an edge of an image. When used in the context of level set segmentation, it has the effect of reducing the propagation speed near an edge in the image where the gradient is high. By suitably changing the value of λ , we can control the strength of the edges that cause the speed to become zero near an edge. With this definition of the speed F , the level set equation can be written as

$$\frac{\partial\phi}{\partial t} = g(x, y)\|\nabla\phi\|\left(\operatorname{div}\left(\frac{\nabla\phi}{\|\nabla\phi\|}\right) + F_0\right). \quad (4)$$

Further modifications to the speed term have been proposed by several authors. For example Yezzi et al.^{17, 18} observe that the stopping factor given by Equation (2) will not force the front to stop at an edge unless it is exactly zero, a situation that rarely occurs in realistic images. They propose adding an additional term of the form $(\nabla g \cdot \nabla\phi)$ to the right-hand side of Equation (4) resulting in the following equation for the evolution of the level set:

$$\frac{\partial\phi}{\partial t} = g(x, y)\|\nabla\phi\|\left(\operatorname{div}\left(\frac{\nabla\phi}{\|\nabla\phi\|}\right) + F_0\right) + \nabla g \cdot \nabla\phi. \quad (5)$$

Since the edge can be defined as a step function, and ∇g involves two derivatives of the image, the term ∇g acts as a ‘‘doublet’’ near an edge. It has the effect of attracting the evolving contour as it approaches an edge and then pushing the contour back out if it should pass the edge. This additional term is called the pullback term or the edge strength stopping force multiplier. Note that with the addition of the doublet term, $(\nabla g \cdot \nabla\phi)$, the level set equation (5) becomes equivalent to the geodesic snake model that was proposed simultaneously by Caselles et al.¹⁹ and Kichenassamy et al.¹⁷

2.2. The placement of the initial contour

A key challenge in both implicit active contours and snakes is the placement of the initial contour. Since the contour moves either inward or outward, its initial placement will determine the segmentation that is obtained. For example, if there is a single object in an image, an initial contour placed outside the object and propagated inward will segment the outer boundary of the object. However, if the object has a hole in the middle, it will not be possible to obtain the boundary of this hole unless the initial contour is placed inside the hole and propagated outward. It should be noted that more than one closed curve can be used for initialization of the zero-th level set.

In this paper, we investigate two different placements of the initial contour. To obtain the exterior boundaries of image objects, we consider a contour that is just inside the outermost boundary of the image. This curve is then propagated inward towards the desired object boundaries. To obtain the inner boundaries of objects, we start with an initial contour that is centered around an appropriately placed interior pixel of the image. In this instance, the sign of the so-called “balloon force” is changed to generate the necessary outward propagation of the initial contour(s). While these two types of initial curve placements are sufficient to help us investigate the level set approach and compare it with the traditional image segmentation algorithms, they are not sufficient for the segmentation of a general image. Alternatives that have been proposed include an initial segmentation based on seeds identified in the image followed by region merging to merge small regions.²⁰

2.3. Calculation of the distance function

Once the initial contour has been determined, we need to calculate the signed distance function ϕ , that is, the minimum distance from each pixel in the image to the prescribed initial contour. This is done by solving the Eikonal equation.^{3,7} This is derived from the level set formulation as follows. Suppose the speed function F is greater than zero. As the front moves outward, one way to characterize the position of the front is to compute the arrival time $T(x, y)$ as it crosses each point (x, y) . This arrival function is related to the speed by

$$\|\nabla T\|F = 1 \tag{6}$$

where $T = 0$ is the initial contour. When the speed F depends only on the position, Equation (6) is referred to as the Eikonal equation. The solution of this equation for a constant speed of unity gives the distance function. The sign is attached to the function depending on the location of each pixel relative to the original contour. In our work, we used the fast sweeping method to solve the Eikonal equation as described by Zhao.²¹

As the front evolves, the signed distance function can often lose the “distance property”.²² As a result, when the curve stops evolving near an edge, the zero level set is not exactly at the edge. One solution to this problem is to periodically re-initialize the distance function ϕ . We use the same Eikonal equation solver for this purpose. However, it should be noted that this can add significantly to the overall computational cost of the level set approach.

2.4. The discretization of the level set equation

In order to evolve the level set equation, Equation (5), must be solved on the discrete grid represented by the image. Here, we borrow extensively from the work that has already been done in the area of the solution of partial differential equations through techniques such as finite difference methods.¹³

The finite difference approach essentially considers the discretized version of the image $I(x, y)$ to correspond to the intensity at the pixels (i, j) , at locations (x_i, y_j) , where $i = 1, \dots, N$, and $j = 1, \dots, M$. The distance between the centers of the pixels, referred to as the grid spacing, is h . The same inter-pixel distance h is used along the x and y dimensions.

Following the approach of Sethian³ (page 73), the level set equation (5) can be written as

$$\frac{\partial \phi}{\partial t} = g(x, y) \|\nabla \phi\| \operatorname{div} \left(\frac{\nabla \phi}{\|\nabla \phi\|} \right) + F_0 g(x, y) \|\nabla \phi\| + \nabla g \cdot \nabla \phi \quad (7)$$

The first term on the right hand side is the curvature term and is the parabolic contribution to the equation. This is discretized using a second-order accurate central difference scheme described by Weickert.⁸ The second term is the hyperbolic propagation term and is discretized using the first-order accurate upwind differencing scheme given in Sethian.³ The third term is a pure advection term and is also discretized using a similar first-order accurate upwind differencing scheme.

When the Equation (5) is evolved using an explicit time integration scheme, such as the forward Euler scheme, the time step size needs to be bounded in order to maintain the numerical stability. In general, the stability restrictions imposed by the parabolic terms tend to be significantly more restrictive than those imposed by the hyperbolic terms. To alleviate this overly restrictive stability criteria, the time integration of the parabolic term is carried out using an implicit scheme with additive operator splitting (AOS).⁸

3. TRADITIONAL METHODS FOR IMAGE SEGMENTATION

In this paper, we compare the performance of the implicit active contour method for segmentation with two of the more traditional techniques, namely the Canny edge detector⁹ and the SUSAN edge detector.¹⁰ The Canny edge detector was chosen in light of its popularity and ease of implementation. It can be considered as a representative gradient-based technique. The SUSAN edge detector was chosen as it is very different from the well known methods in that it uses no image derivatives and noise reduction is needed.

The Canny edge detector detects edges at the zero crossings of the second directional derivative of the smoothed image in the direction of the gradient, where the gradient magnitude is above some threshold. The implementation of the Canny edge detector used in this paper first smooths the image using a Gaussian with standard deviation σ . Next, a Sobel edge detector²³ is applied to the smoothed image and the magnitude and direction of the gradient are calculated at each pixel. This is followed by non-maximal suppression, where only the pixel with the largest magnitude along the direction of the gradient is retained for further processing. This results in a thinning of the edges found by the Sobel operator. Finally, a hysteresis thresholding is applied with two thresholds - t_{lo} and t_{hi} . All edge pixels with gradient magnitude less than t_{lo} are discarded while those with gradient magnitude larger than t_{hi} are retained. Edge pixels with gradient magnitude in between the two thresholds are retained only if they have a neighboring pixel with gradient magnitude greater than t_{hi} . As this process is applied recursively, such pixels are retained if they are connected to a pixel with gradient magnitude greater than t_{hi} , either directly, or indirectly through other pixels with a gradient magnitude between the two thresholds. Thus, our implementation of the Canny edge detector requires three parameters: σ , t_{hi} , and t_{lo} .

The SUSAN edge detector is based on the Smallest Univalued Segment Assimilating Nucleus principle. A circular mask of a given size, whose center pixel is referred to as the “nucleus”, is placed over each pixel in the image. If the brightness of the pixels that lie under the mask is within a threshold, t , of the brightness of the nucleus, then an area of the mask can be defined which has a brightness similar to the nucleus. This area is referred to as the USAN (Univalued Segment Assimilating Nucleus) and contains information about the structure of the image. The USAN area is at a maximum when the nucleus lies in a region of uniform brightness, it falls to half the maximum near an edge, and falls even further when at a corner. The threshold t is the minimum contrast of the image features that will be detected and also the maximum amount of noise that will be ignored. the area of the USAN is compared with $0.75 * (\text{the maximum area})$, and an initial edge response is calculated that is proportional to this difference. The 0.75 scale factor in the comparison is selected to give optimal noise rejection. This original implementation of the SUSAN principle has since been modified to yield a more stable implementation. More details are available in the article by Smith and Brady¹⁰ and the source code is available on-line at www.fmrib.ox.ac.uk/~steve.

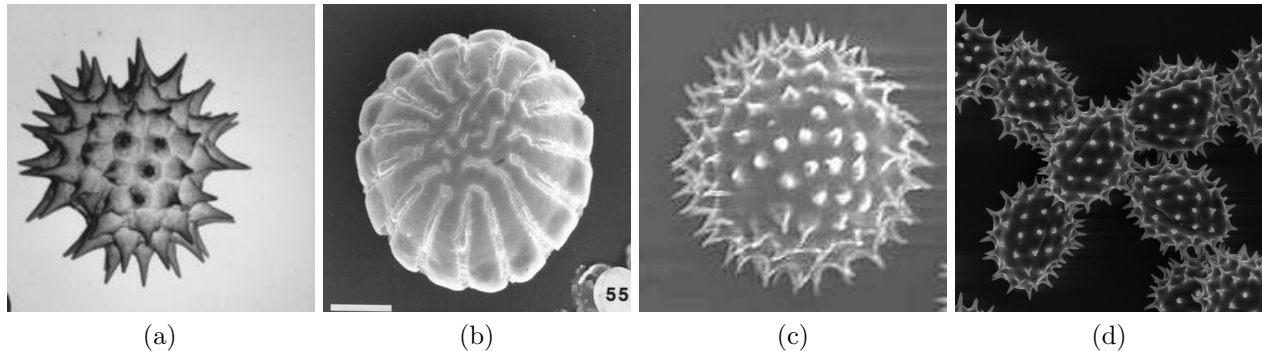


Figure 1. Original Scanning Electron Microscope images of pollen. Panels (a) and (b) are from the pollen.usda.gov site, while panels (c) and (d) are from the www.cci.ca.gov/Reference website.

4. COMPARISON OF TECHNIQUES

In this section, we describe the results of our experiments with segmentation using the implicit active contour approach and compare it with the more traditional techniques such as the Canny and SUSAN edge detectors. In particular, we are interested in understanding how the implicit active contour performs relative to the more established segmentation techniques and what benefits are obtained for the additional computations that are required by the level set approach. In this paper, we will compare the results of segmentation visually on the experimental images.

4.1. Experimental images

For our work, we have chosen scanning electron microscope images of pollen. Pollen grains typically have a complex structure with sharp spines or an intricate web like pattern. If we are interested in automatically finding out how many pollen grains of each type are present in an image, we first need to segment the image to find the individual pollen grains, and then perform pattern recognition to classify them into different categories. The latter can be done perhaps by using the internal texture of the grains or by extracting features from the boundary such as the size and curvature of the spines.

In order to evaluate the different segmentation methods, we have chosen four test images (see Figure 1). The images in panels (a) and (b) are of a single pollen grain. These were obtained from the pollen.usda.gov site. The images in panels (c) and (d) were obtained from the www.cci.ca.gov/Reference website. Panel (c) is the image of a single pollen grain, while panel (d) has several pollen grains. These images were selected to investigate the issues in segmenting images with high curvature (as in the sharp spines), or images with poor contrast (panel (b)), or images with poor quality (panel (c)), as well as images with more than one pollen grain (panel (d)).

All images in the study were used without any modification. However, contrast enhancement or sharpening of the images may be necessary in some cases to improve the quality of segmentation.

4.2. Experimental Results and Observations

We first present the results of our experiments with the implicit active contour approach. Figure (2) shows the results of the segmentation of the test images. In each case, the balloon force was set to ± 7.5 , with the sign determining whether the contour moved inward from the edge of the image to segment the outer boundary or outward from a point in the center of the image to segment the inner structure. No reinitialization was used. Unless stated otherwise, the level set is evolved for 2000 iterations. If the parameters for the level set approach are selected correctly, we expect the level set to stop evolving once it has reached the boundary.

The zero-th level set contour in Figure (2) is highlighted in white. Panel (a) shows the result of the outer boundary detection. The contrast of the image makes it difficult to see the contour, which is right at the outside

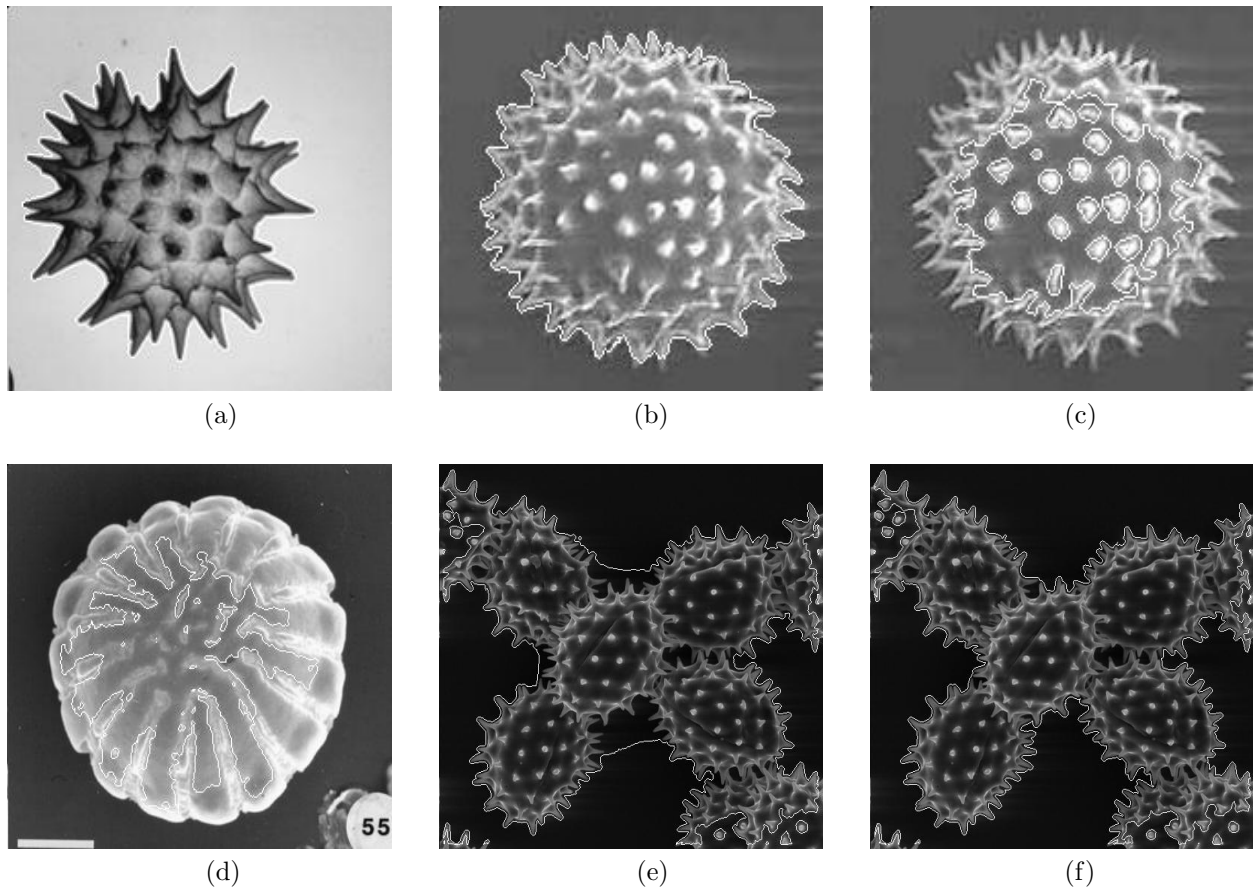


Figure 2. Output of the implicit active contour edge detector: All images were segmented using a balloon force ± 7.5 , with the sign depending on whether the inside or outside of the pollen grain is being segmented. Panels (a), (b), and (c) were obtained with no reinitialization and no doublet term. Panels (a) and (b) were obtained at iteration 2000, while Panel (c) was initialized at a point in the center of the pollen grain and shows the results after 5000 iterations. Panel (d) uses no reinitialization, but the doublet term was set to handle the low contrast structures. The results are shown at iteration 3500. Panels (e) and (f) are with no reinitialization at iterations 300 and 500 and show the evolution of the level set.

boundary. Another similar image is shown in panel (b), where the segmentation of the outer boundary is clearly visible. Panel (c) is the same image as panel (b), with the initial contour selected as a point inside the pollen grain. Since the internal structure is very complex, we present the results after 5000 iterations. Panel (d) shows the results of segmenting the internal structure in an image with low contrast. The results are shown after 3500 iterations. Since the contrast is poor, we use the doublet term to prevent the level set from breaking through the fine structure. However, given the values used for the different parameters, the level set does break through the poor contrast regions, and approaches the outer boundary as it is evolved further. In panels (e) and (f), we show the evolution of the zero-th level set as it moves inward from the outer boundary of the image to segment multiple objects.

In the experiments reported in this study, we set the parameters in Eqn (2) to $\sigma = 0.5$ and $\lambda = 1.0$.

In the next experiment, we focused on the image in Figure (1), panel (a) in order to better understand the effects of reinitialization and the addition of the doublet term (Eqn. (5)). Figure (3) shows a small corner

of the pollen grain to illustrate the evolution of the active contour. The results are shown at iteration 500, 1000, and 1500, respectively. For the images in the first column which are generated without reinitialization, we observe that the curve stops at the boundary. With reinitialization every 10 time steps (images in column 2), the curve breaks through the edge and continues to evolve. The addition of the doublet term, as shown by the images in column 3, prevents the breakthrough. These images were generated using a balloon force of -7.5 (the negative sign indicates that the curve should evolve inwards). The original contour is placed just inside the outer boundary of the image. As in the earlier experiment, the values of the parameters in Eqn (2) are set to $\sigma = 0.5$ and $\lambda = 1.0$.

We next present the results obtained with the Canny edge detector in Figure (4). The values of the parameters used were $\sigma = 1.0$, $t_{lo} = 64$, and $t_{hi} = 128$. The edges are overlaid on the images in black. For the image with the poor contrast (Figure (1), panel (b)), we found that a smaller value of $\sigma = 0.1$ resulted in less smoothing of the image and thus better detection of the edges. Similarly, a lower value of $t_{lo} = 32$ resulted in more edges being detected.

Figure (5) shows the results obtained with the SUSAN edge detector. We experimented with values of the brightness threshold set to 20 and 40. We found that we obtained better results with threshold of 20 used for both the initial smoothing and the edge detection. The edges are indicated in the images by a black pixel.

4.3. Observations

While this is a preliminary study, there are several observations we can make about the pros and cons of the methods considered. Both the SUSAN and Canny edge detectors are computationally very efficient and required the setting of just a few parameters. In contrast, the implicit active contours are computationally very expensive. It also requires the setting of several parameters such as the strength of the balloon force, the parameters σ and λ in Eqn (2), the number of time steps before reinitialization, the placement of the initial contour, and whether to use the doublet term or not. As with the Canny and SUSAN edge detectors, some of these parameters have to be tuned to the image and the type of structure we want to segment. However, the active contour approach does have a very appealing quality that it generates closed contours, thus eliminating the tedious post-processing that is needed to convert the edges from the SUSAN or the Canny edge detectors into closed boundaries of an object.

5. SUMMARY AND FUTURE WORK

This paper outlines a preliminary study of the use of the implicit active contour approach for image segmentation and compares it with the traditional approaches such as the Canny and the SUSAN edge detectors. We observed that while the active contour approach is computationally expensive and requires the setting of several parameters, it generates closed contours, which can be very useful in separating the outer boundaries of an object from the background. Our future work includes a more detailed study of the different parameters to understand the sensitivity of the algorithm to the values of these parameters, a comparison of the quality of the edges obtained by different methods, as well as the use of other scientific images. We are also interested in exploring combinations of these active contour techniques with the traditional edge detectors to see if we can combine the positive aspects of the different approaches.

ACKNOWLEDGMENTS

This work was performed under the auspices of the U.S. Department of Energy by University of California Lawrence Livermore National Laboratory under contract No. W-7405-Eng-48.

REFERENCES

1. G. Sapiro, *Geometric Partial Differential Equations and Image Analysis*, Cambridge University Press, 2001.
2. G. Aubert and P. Kornprobst, *Mathematical Problems in Image Processing: Partial Differential Equations and the Calculus of Variations*, Springer-Verlag, 2002.

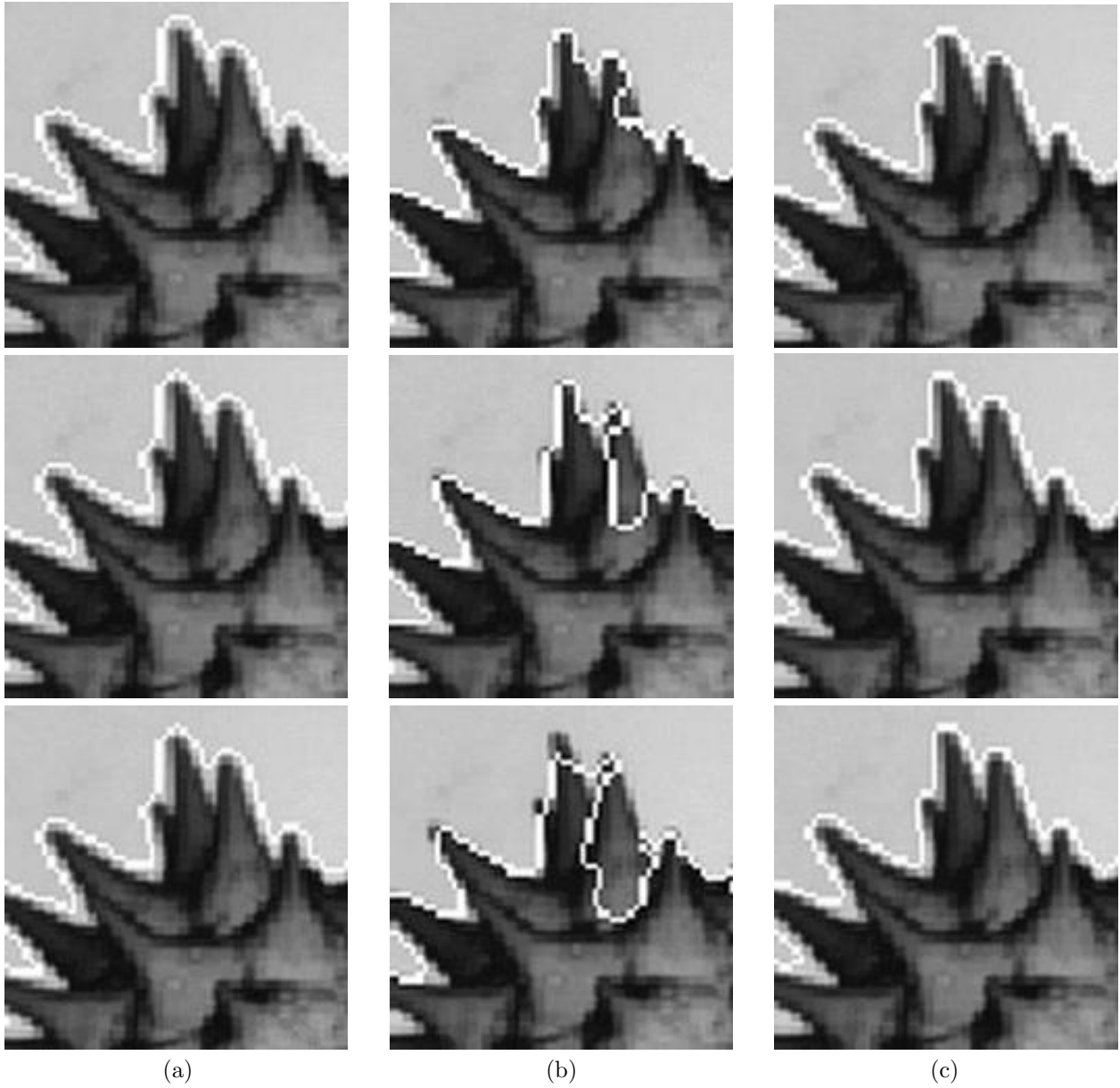


Figure 3. Evolution of the implicit active contour for Figure (1), panel (a): The three rows are at iteration 500, 1000, and 1500, respectively. The images in column (a) are without reinitialization and without the use of the doublet term. The images in column (b) are with reinitialization every 10 time steps, but without the use of the doublet term. Note that the contour breaks inside the boundary and continues to evolve. Column (c) is with reinitialization and with the use of the doublet term. Note that the doublet term prevents the contour from breaking through the edge.

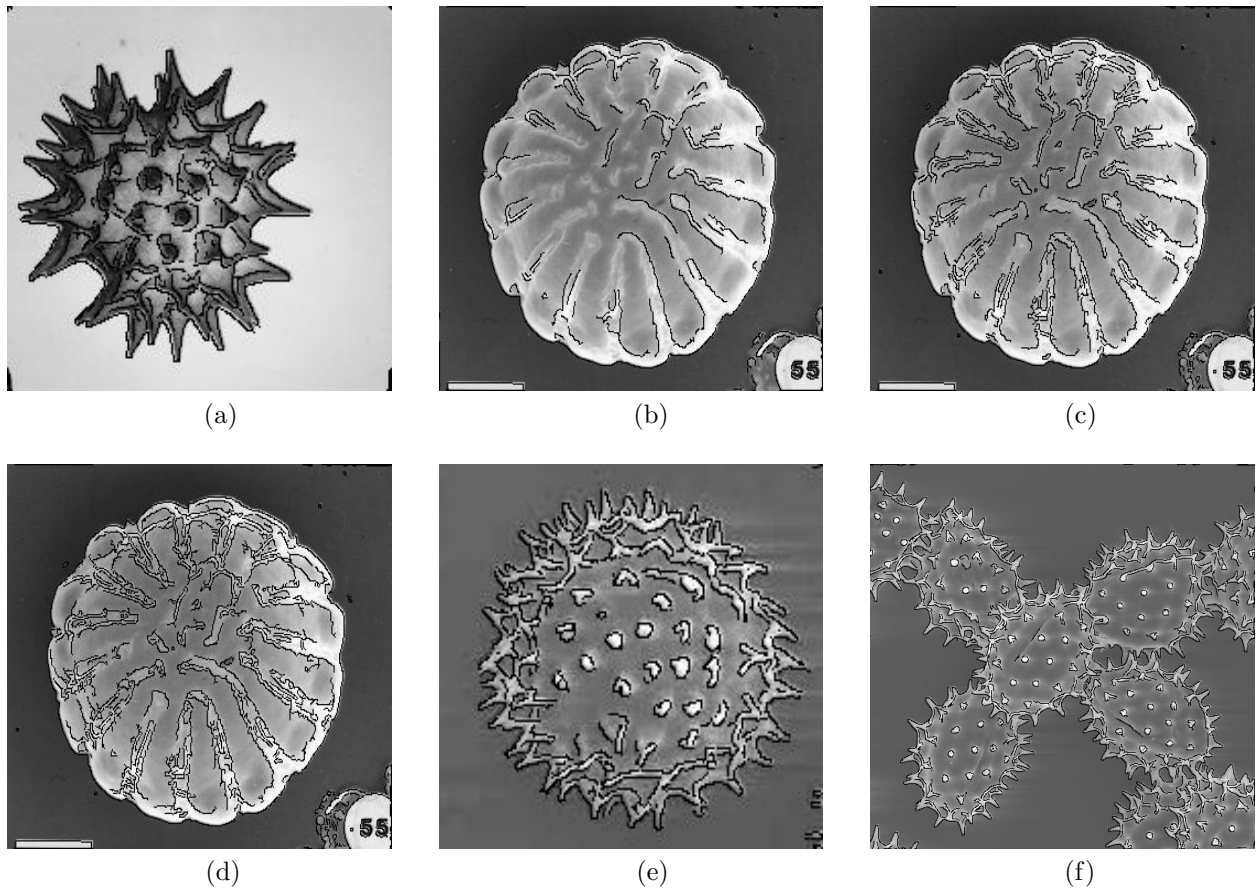
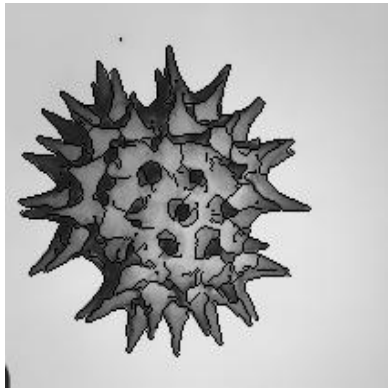
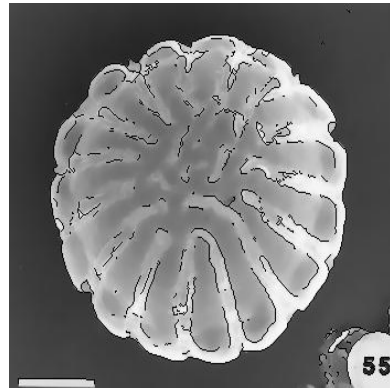


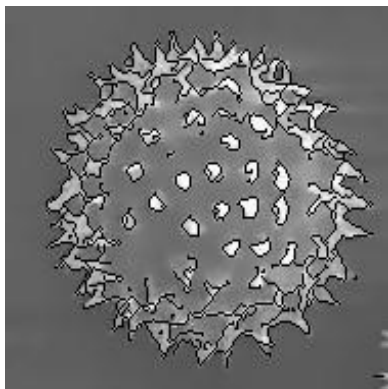
Figure 4. Output of Canny edge detector: All images are generated using $\sigma = 1.0$, $t_{lo} = 64$, and $t_{hi} = 128$. Panel (c) uses $\sigma = 0.1$ and panel (d) uses $\sigma = 0.1$ and $t_{lo} = 32$. The contrast in Panel (f) has been changed to better highlight the edges.



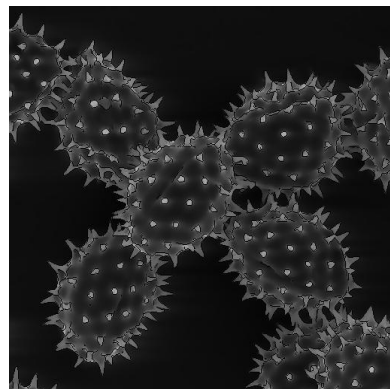
(a)



(b)



(c)



(d)

Figure 5. Output of the SUSAN edge detector: All images are generated by first smoothing the image with a threshold of 20, followed by edge detection with a brightness threshold of 20.

3. J. Sethian, *Level Set Methods and Fast Marching Methods: Evolving Interfaces in Computational Geometry, Fluid Mechanics, Computer Vision, and Materials Science*, Cambridge University Press, 2003.
4. R. Malladi, *Geometric methods in Bio-Medical Image Processing*, Springer, 2002.
5. S. Osher and N. Paragios, *Geometric Level Set Methods in Imaging, Vision, and Graphics*, Springer-Verlag, 2003.
6. S. Osher and R. Fedkiw, *Level Set Methods and Dynamic Implicit Surfaces*, Springer-Verlag, 2003.
7. J. Suri, L. Liu, S. Singh, S. Laxminarayan, X. Zeng, and L. Reden, "Shape recovery algorithms using levels sets in 2-D/3-D medical imagery: A state-of-the-art review," *IEEE Transactions on Information Technology in Biomedicine* **6**(1), 2002.
8. J. Weickert and G. Kühne, "Fast methods for implicit active contour models," technical report, preprint no. 61, Universität des Saarlandes, 2002.
9. J. Canny, "Finding edges and lines in images," Master's thesis, MIT, Cambridge, Massachusetts, 1983.
10. S. Smith and J. Brady, "SUSAN - a new approach to low-level image processing," *International Journal of Computer Vision* **23**(1), pp. 45–78, 1997.
11. S. Osher and J. A. Sethian, "Fronts propagating with curvature dependent speed: Algorithms based on Hamilton-Jacobi formulations," *Journal of Computational Physics* **79**, pp. 12–49, 1988.
12. J. A. Sethian, "Tracking interfaces with level sets," *American Scientist* **85**(3), 1997.
13. V. Vemuri and W. J. Karplus, *Digital Computer Treatment of Partial Differential Equations*, Prentice Hall, 1981.
14. R. Malladi, J. Sethian, and B. Vemuri, "Shape modelling with front propagation: A level set approach," *IEEE Transactions on Pattern Analysis and Machine Intelligence* **17**(2), pp. 158–175, 1995.
15. K. Siddiqui, Y. Lauzière, A. Tannenbaum, and S. Zucker, "Area and length minimizing flows for shape segmentation," *IEEE Transactions on Image Processing* **7**(3), pp. 158–175, 1998.
16. P. Perona and J. Malik, "Scale-space and edge detection using anisotropic diffusion," *IEEE Transactions on Pattern Analysis and Machine Intelligence* **12**(7), pp. 629–639, 1990.
17. S. Kichenassamy, A. Kumar, P. Olver, A. Tannenbaum, and A. Yezzi, "Gradient flows and geometric active contour models," in *Proceedings, IEEE Fifth International Conference on Computer Vision*, pp. 694–699, 1995.
18. A. Yezzi, S. Kichenassamy, A. Kumar, P. Olver, and A. Tannenbaum, "A geometric snake model for segmentation of medical imagery," *IEEE Transactions on medical imaging* **16**(2), pp. 199–209, 1997.
19. V. Caselles, R. Kimmel, and G. Sapiro, "Geodesic active contours," in *Proceedings, IEEE Fifth International Conference on Computer Vision*, pp. 694–699, 1995.
20. Z. Yu and C. Bajaj, "Normalized gradient vector diffusion and image segmentation," in *Proceedings of 7th European Conference on Computer Vision*, **3**, pp. 517–530, 2002.
21. H. Zhao, "A fast sweeping method for Eikonal equations," Technical report, Department of Mathematics, University of California, Irvine, 2003. To appear in Math Comp. Online version available at www.math.uci.edu/~zhao/publication/publication.html.
22. J. Gomes and O. Faugeras, "Reconciling distance functions and level sets," *Journal of Visual Communication and Image Representation* **11**, pp. 209–223, 2000.
23. M. Sonka, V. Hlavac, and R. Boyle, *Image Processing, Analysis, and Machine Vision*, PWS Publishing, 1999.